The Dipole Mediated Surface Chemistry of *p*-Benzoquinonemonoimine Zwitterions

Peter A. Dowben · Donna A. Kunkel ·
Axel Enders · Luis G. Rosa · Lucie Routaboul ·
Bernard Doudin · Pierre Braunstein

Abstract This article reviews the surface adsorption of *p*-benzoquinonemonoimine zwitterions from the class of *N*-alkyldiaminoresorcinones (or 4,6-bis-dialkylamino-benzene-1,3-diones, i.e. $C_6H_2(\cdots NHR)_2(\cdots O)_2$), where R = H, R = C_2H_5, n-C_4H_9), on a variety of conducting surfaces. These small molecules with a large electrical dipole exhibit molecular orientation and packing on surfaces depending on the deposition methodology (from solution or from the vapor) as well as the substrate. What is very clear from the investigations of this class of molecules is that inter-molecular interaction is not simply driven by dipolar interactions alone, but frontier orbital symmetry as well. This is illustrated by the reversible adsorption of di-iodobenzene on molecular films of (6Z)-4-(butyla-mino)-6-(butyliminio)-3-oxocyclohexa-1,4-dien-1-olate $C_6H_2(\cdots NHR)_2(\cdots O)_2$ where R = n-C_4H_9, where it is clear that absorption is isomer specific.

1 Introduction

This short review presents our recent results on substrates functionalization with thin films made of molecules with large intrinsic dipole to investigate the interplay between dipolar interactions and the influence of the frontier molecular orbitals. We have used the zwitterion thin films for investigating reversible adsorption of weakly adsorbed molecules [1] to show that the interactions between molecules with a large intrinsic dipole are mediated by more than just a summation of classical electrostatic forces, i.e. the Topping model [2] is far from complete. In some sense,

P. A. Dowben (✉) · D. A. Kunkel · A. Enders · L. G. Rosa
Department of Physics and Astronomy, Nebraska Center for
Materials and Nanoscience, University of Nebraska-Lincoln,
Theodore Jorgensen Hall, 855 North 16th Street, Lincoln,
NE 68588-0299, USA
e-mail: pdowben@unl.edu

A. Enders
e-mail: aenders2@unl.edu

L. G. Rosa
e-mail: luis.rosa13@upr.edu

L. G. Rosa
Department of Physics and Electronics, University of Puerto
Rico-Humacao, Av. Jose E. Aguiar Aramburu Road 908 CUH
Station, Humacao, PR 00791, USA

L. G. Rosa
Institute for Functional Nanomaterials,
University of Puerto Rico, Facundo Bueso Building,
Rio Piedras, PR 00931, USA

L. Routaboul · P. Braunstein
Laboratoire de Chimie de Coordination, Institut de Chimie
(UMR 7177 CNRS), 4 Rue Blaise Pascal, Université de
Strasbourg, 67081 Strasbourg, France
e-mail: braunstein@unistra.fr

B. Doudin
Institut de Physique et Chimie des Matériaux de Strasbourg,
IPCMS (UMR 7504), Université Strasbourg, 23 Rue du Lœss,
B.P. 20, 67034 Strasbourg, France
e-mail: bdoudin@unistra.fr

the study of adsorbate dipolar molecules is an extension of investigations where molecular adsorption has been shown to depend on the polarization ferroelectric domain orientation of both organic [2–7] and inorganic ferroelectrics [8–28]. Such studies have largely investigated polar adsorbate molecules [2–13], with the tacit assumption that nonpolar molecules should be insensitive to the ferroelectric polarization domain orientation [8–10]. The chemistry of the surface can play a role and one can expect that the surface chemistry of positive and negative ferroelectric domains are not identical [7, 14, 15]. In this sense, nonpolar molecules would not be immune from the surface dipole direction of a ferroelectric surface. Not only would the nonpolar molecule respond to the dipole direction, as all molecules have a finite polarizability, but the termination, stoichiometry and defect densities of a surface can differ with different dipole (polarization) directions. Highlighting this complexity, we have found that the adsorption of di-iodobenzene on the molecular ferroelectric copolymer polyvinylidene fluoride with trifluoroethylene (70:30) is sensitive to the polymeric ferroelectric domain orientation, but varies also with isomer [7]. Both polar and nonpolar isomers of di-iodobenzene are influenced by the substrate dipole direction: 1,4-(para)di-iodobenzene adsorption at 150 K strongly favors a positive ferroelectric domain orientation while the 1,2-(ortho)di-iodobenzene adsorption at 150 K strongly favors a negative ferroelectric domain orientation with regard to adsorption on the ferroelectric copolymer polyvinylidene fluoride with trifluoroethylene. This polarization direction sensitivity of a nonpolar molecule does suggest that the surface chemistry that accompanies a change in dipole direction does matter. But can it be shown that the frontier orbitals can "trump" the dominant role of dipolar interactions in the chemistry at the hetero-molecular interface? Obviously this is a somewhat rhetorical question because the point of this review is that the answer is an unequivocal "yes".

While the dipolar interaction for an adsorbate on a conducting substrate is a competition between molecule–substrate and molecule–molecule interactions [29, 30], the interactions based on intermolecular dipolar interactions harken back to the problem of the cavity field introduced by Lars Onsager [31]. Onsager's concept of the "cavity field" describes the effective internal field in polar liquids. The cavity field can orient molecules in the ferroelectric phase, and the molecules then polarize the nearby neighbor molecules. This in turn generates a reaction field. With adsorption on a ferroelectric, there are some significant differences from Onsager's cavity field concept as there is an effective external field provided by the ferroelectric substrate acting on the adsorbate molecules with a strong dipole, but the reaction field concept is retained. Is the substrate–molecule dipolar interaction a result of the local

field induced by the substrate or is it caused by image dipole within the substrate generated by a dipolar adsorbate molecule on a conducting substrate? The answer to this dilemma is complicated by the interplay of competing interactions. So a simple model of dipole interactions may not in fact be so "simple" making a picture like that of Topping [2] invalid.

The quinonoid zwitterions that we investigated, although electrically neutral as a whole, carry positive and negative charges on different parts of the molecule (Fig. 1). The positive charge is delocalized between the nitrogen functions over four bonds involving 6π electrons, while the negative charge is spread likewise between the oxygen atoms [32–34]. The result is a large electric dipole that is formed across the planar six-membered ring of the benzoquinonemonoimine "core". These two 6π systems are connected by two carbon–carbon σ-bonds but are electronically not conjugated. The large dipole makes these zwitterionic compounds fascinating candidates for the study of adsorbate dipole interactions at conducting and non-conducting substrate interfaces [1, 7, 29, 35–38]. Those shall be reviewed here, with focus on the zwitterionic p-benzoquinonemonoimine compounds of Fig. 1.

2 Coplanar Dipole Mediated Packing of the p-Benzoquinonemonoimine Zwitterions on Metallic Surfaces

Two-dimensional arrangements of large adsorbates with strong electric dipoles can exhibit strong intermolecular interactions [28, 39–42]. A key role is played by the substrate, because it can enhance or suppress dipole–dipole interactions between organic adsorbates through interface interactions [28, 30, 43]. The result is that with the adsorption of molecules with a large intrinsic electric dipole, the interaction with the substrate can change the interface dipole through several effects such as charge transfer, mirror dipoles and surface-enhanced dipole moments, and this in turn can strongly affect the dipolar interactions of an adsorbate such as the p-benzoquinonemonoimine zwitterions [29].

A scanning tunneling microscopy (STM) image of the p-benzoquinonemonoimine zwitterion **1** adsorbed on a crystalline Cu(111) surface is shown in Fig. 2, along with the proposed structural model. The molecules form one-dimensional, "zipper-like" chains oriented along the ⟨1-10⟩ directions of the surface. The alignment of the molecules within the chains with alternating orientation is reminiscent of arrangements at the solid–liquid interface on graphite [38] and in bulk crystals [32, 37], albeit on surfaces the molecules lie almost flat.

Fig. 1 Zwitterion *p*-benzoquinonemonoimine compounds from the class of *N*-alkyldiaminoresorcinones i.e., $C_6H_2(NHR)_2(O)_2$, where R = H (**1**), R = C_2H_5 (**2**), *n*-C_4H_9 (**3**)
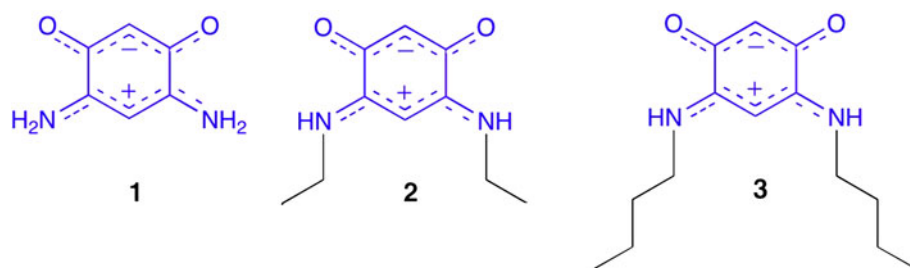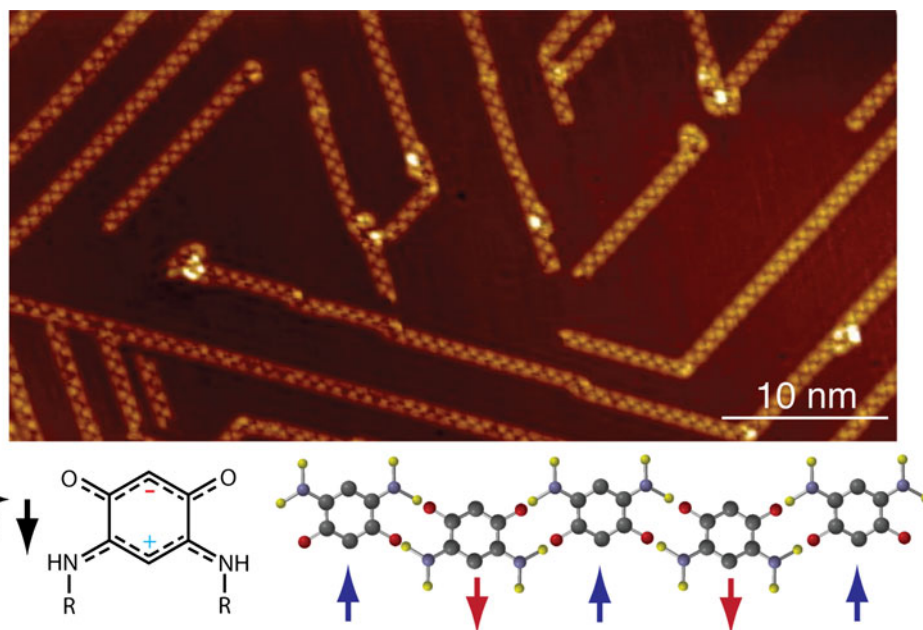
Fig. 2 (*top*) STM image of adsorbed parent quinonoid zwitterion **1** on Cu(111). Tunneling parameters—0.5 V, 300 pA. (*bottom*) Structure model of the one-dimensional chains and the orientation of the intrinsic dipoles. (color code: oxygen-*red*, carbon-*grey*, nitrogen-*blue*, hydrogen-*yellow*). Adapted with permission from [29]. Copyright (2012) the Royal Society of Chemistry

The same molecules deposited on Ag(111) [29] and Au(111) exhibit a very different self-organization at a similar sub-monolayer coverage. The *p*-benzoquinonemonoimine zwitterion **1** will condense into highly ordered 2D networks as seen in Figs. 3a and 4 for Ag(111) and Au(111), respectively. Islands of *p*-benzoquinonemonoimine zwitterion **1** adsorbed on crystalline Ag(111) surface show structural domains exhibiting a unit cell of nearly square shape [29], along with many other similarities to the packing on Au(111). Adjacent domains are separated by boundaries, such as those highlighted in Figs. 3c and 4c. STM images of the zwitterion **1** on Au(111) are shown in Fig. 4a, b. On Au(111) these molecules nucleate preferentially in the regions between the well-known herringbone reconstructions [44], which are also visible in Fig. 4a. The Au(111) surface reconstruction does not impede island growth of the zwitterion (Fig. 4a). As the coverage increases, the zwitterion networks form large islands extending over many herringbone ridges. As with zwitterion **1** on Ag(111) [29], on Au(111) the functional nitrogen groups of each molecule bind to the oxygen of two neighboring molecules via charge-assisted hydrogen bonds.

This bonding scheme implies parallel alignment of the dipole moments of the molecules within each island, which gives the islands remnant electric polarization.

The parallel moments packing depends on the substrate and also on the length of the *N*-substituent. Similar 2D networks but without any domain boundaries are observed if the somewhat larger *N,N'*-diethyl derivatives of the *p*-benzoquinonemonoimine zwitterion **2** is adsorbed on crystalline Ag(111) (Fig. 3b). The appearance of the molecules, and their measured nearest neighbor separation when adsorbed from the vapor on Ag(111) and Cu(111) [29] is consistent with the molecules lying flat on the surface and with the published spacing of quinones on HOPG [38] as well as the crystallographic data of the bulk [32, 37]. Interestingly, while the packing of the various *p*-benzoquinonemonoimine zwitterions on graphite [38] and in the bulk [32, 37] shows the general tendency to minimize the overall net dipole, this is not observed in the packing structures adopted on Ag(111). We note further that related zwitterions attach to the substrate in a standing-up orientation when deposited from solution with higher coverage [32, 37], as will be discussed below.
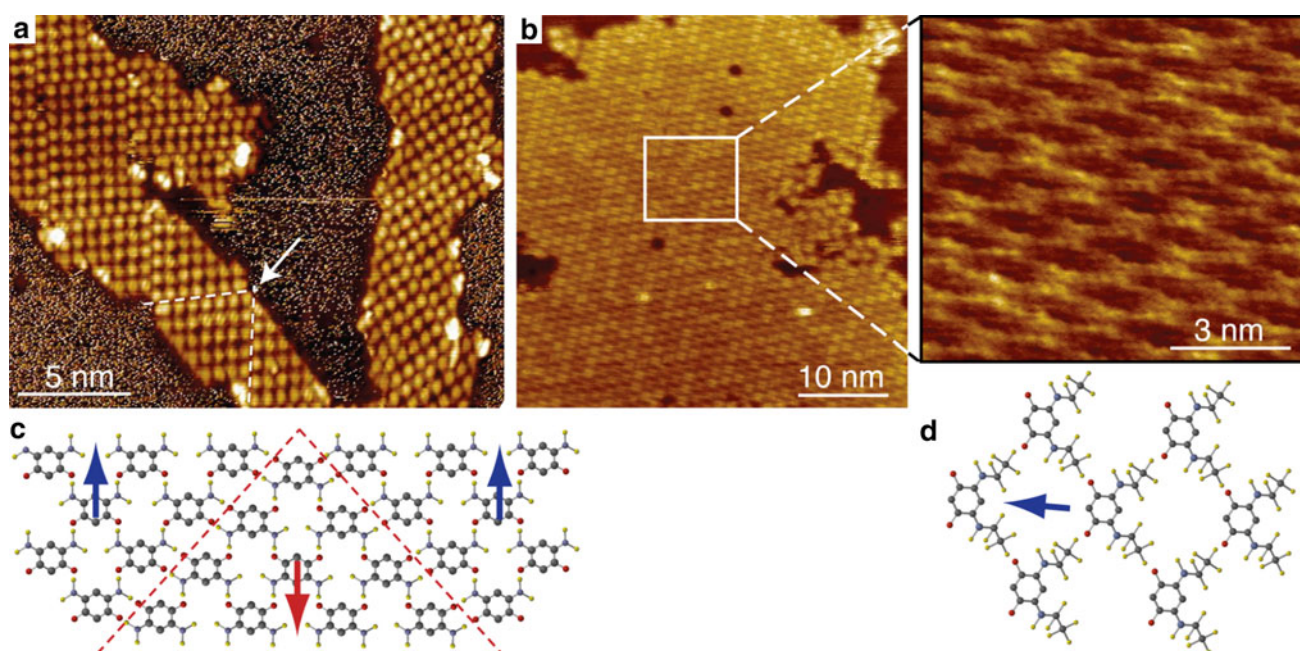
Fig. 3 a The STM image of *p*-benzoquinonemonoimine zwitterion **1** on Ag(111). White dashed lines mark the boundaries between selected structural domains. **b** the *p*-benzoquinonemonoimine zwitterion **2** on Ag(111), with close-up image. **c** Structure model of

p-benzoquinonemonoimine zwitterion **1** adlayer structure (**a**). **d** Structure model of the *p*-benzoquinonemonoimine zwitterion derivative **2** in (**b**). Adapted with permission from [29]. Copyright (2012) the Royal Society of Chemistry
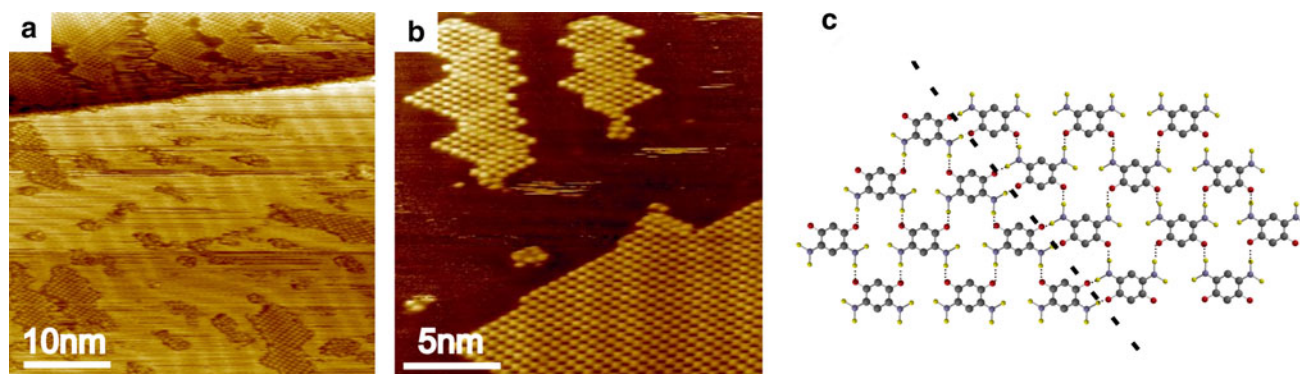

Fig. 4 a The STM topography of the quinonoid zwitterion **1** on Au(111). Tunneling parameters—0.7 V, 250 pA **b** A zoom in of self-assembled networks on Au(111), STM topography imaged at −0.3 V,

300 pA. **c** Proposed bonding of zwitterions on Au(111) showing two domains of aligned molecules separated by a *dashed line*. *Gray* represents C, *yellow* H, *red* O, and *blue* N

What is striking is the difference in the bonding patterns and resulting polarization of the zwitterion adsorbate structures. The polarization is zero for the zigzags chain like structures formed by the zwitterion **1** adsorbed on Cu(111) [29] and graphite (HOPG) [38] but the in-plane net polarization assumes a maximum for the networks of the somewhat larger *p*-benzoquinonemonoimine zwitterion **2** on Ag(111) [29]. Between both extremes is the *p*-benzoquinonemonoimine zwitterion **1** on Ag(111), which forms a multi-domain electret. The parallel alignment of the dipoles of the zwitterions on Ag(111) and Au(111) is

surprising and would seem to contradict simple electrostatic arguments, as well as the results observed for various *p*-benzoquinonemonoimine zwitterions on graphite. Thus, we conclude that the effective dipole of the supported zwitterions depends on the substrate [29]. While the dipole moment drives the bonding scheme to some extent, overall, there must be interplay of multiple interactions. The Coulomb forces experienced by a molecule is one of those interactions, but it depends on the details of the local electrostatic potential and cannot easily be deduced from the molecular dipole alone.

3 The Adsorption of Di-iodobenzene on *p*-Benzoquinonemonoimine Zwitterion Molecular Films

This interplay between the surface chemical interactions and the electrostatic dipolar interactions can be explored by comparing adsorption of isomeric molecules that are both polar and nonpolar. The investigation of molecular isomeric effects on the adsorption of different di-iodobenzene isomers on molecular zwitterion films demonstrated that the frontier orbital symmetry can play a dominant role in the adsorption process [1]. As discussed above, like the alkane thiols on gold, the *p*-benzoquinonemonoimine zwitterions $C_6H_2(\cdots NHR)_2(\cdots O)_2$ appear to adsorb with the core parallel with the surface when adsorbed on copper [29], silver [29] and gold from the vapor, but orient with the six-membered core perpendicular to the surface when adsorbed from solution [35, 37]. This upright bonding orientation for the zwitterion **3** on gold (Fig. 5) has been confirmed by angle resolved photoemission [35], atomic force microscopy [37], and is consistent with the band structure of the molecular adlayer [37], infrared spectroscopy [35] and core level photoemission [35] spectra. The reason for the zwitterions adsorbing with the 'lying down', with adsorption from the vapor, is partly the lower packing density.

Configuration on graphite [38], as opposed to the upright configuration on gold [35, 37], when the deposition is done from solution on both substrates, likely has much to do with the very weak interaction seen with the *p*-benzoquinonemonoimine zwitterion on graphene [36] and likely graphite as well.

All three isomers of di-iodobenzene adsorb molecularly on 0.5–1 nm thick films of zwitterion **3** with the substrates held at 150 K. The characteristic molecular orbitals of 1,2-di-iodobenzene, 1,3-di-iodobenzene and 1,4-di-iodobenzene are clearly evident in the combined photoemission and inverse photoemission, shown in Fig. 6 for di-iodobenzene adsorption on zwitterion **3** molecular films of identical thickness and preparation. There is, however, no indication of interactions of any of the di-iodobenzene with the underlying Au substrate, confirming previous observations on clean graphite [45] and copper surfaces [46].
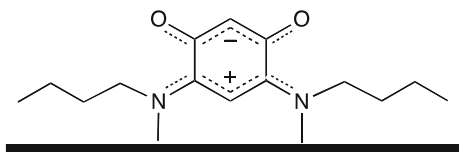
With increasing adsorption of all three isomers of di-iodobenzene on the zwitterion **3** thin films, the apparent HOMO–LUMO gap increases and features appear (Fig. 6) consistent with the molecular orbitals of the pertinent di-iodobenzene. The various isomers of di-iodobenzene actually have a very similar electronic structure, and there is agreement of the single molecule calculations with the combined photoemission and inverse photoemission, as seen in Fig. 6. The combined photoemission and inverse photoemission spectra of the zwitterion **3** molecular films on Au indicate a highest occupied molecular orbital (HOMO) to lowest unoccupied molecular orbital (LUMO) gap of 5.8–6.0 eV for the thinner of the films. These experimental values are consistent with the calculated value of 5.8 eV based on simplistic single molecule semiempirical method NDO-PM3 (neglect of differential diatomic overlap, parametric model number 3) [1].

The adsorption of all of the di-iodobenzene isomers was seen to be reversible with no characteristic molecular orbitals nor any iodine 3D core level signal evident upon annealing to room temperature. There are clear experimental indications that the isomers, while all adsorbing on the zwitterion molecular films, exhibit isomeric dependence. For adsorption on the thinner 1 nm molecular films (of Fig. 5), it was inferred that the sticking coefficient of 1,3-di-iodobenzene on zwitterion **3** molecular films is roughly 3–5 times larger than that observed for 1,4-di-iodobenzene, and 15 times larger than for 1,2-di-iodobenzene adsorption at 150 K [1]. This qualitative trend is even more apparent on thicker (2–3 nm thick) molecular films at 150 K, as detailed in the next section.

From the increase in the $3d_{5/2}$ X-ray photoemission core level iodine signals with exposure time, for di-iodobenzene adsorption on thicker films, it was found that for 1,3-di-iodobenzene the initial kinetic adsorption rates were roughly 70 times larger than observed for 1,2-di-iodobenzene and 210–250 times larger than observed for 1,4-di-iodobenzene at 150 K, as summarized in Fig. 7. Again, we see a strong preference for the adsorption/absorption of 1,3 di-iodobenzene.

Di-iodobenzene adsorption studies on molecular films of zwitterion **3** reveal that 1,3-di-iodobenzene adsorption is strongly favored over the other isomers of di-iodobenzene [1]. Not only is there a far greater sticking coefficient for 1,3-di-iodobenzene adsorption, but there is a far larger core level binding energy shifts (I $3d_{5/2}$ decreasing from 621.9 ± 0.2 eV to 619.4 ± 0.1 eV) with increasing 1,3-di-iodobenzene coverage values. This finding suggests that this isomer favors strong π–π interactions with the adjacent molecules **3**. This isomer of di-iodobenzene shares the same symmetry as the C_6 core of the *p*-benzoquinonemonoimine zwitterion compound, suggesting that the frontier molecular orbital symmetry plays a dominant role in

Fig. 5 The suggested interaction configuration of the zwitterion **3** when deposited on gold from solution. See [35] for details
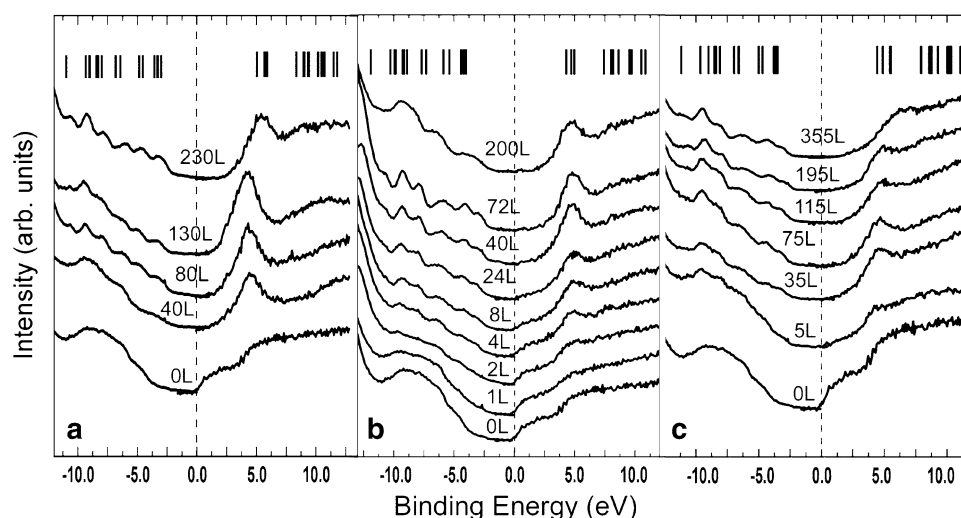
Fig. 6 The combined photoemission and inverse photoemission of 1 nm thick zwitterion **3** molecular films as a function of **a** 1,2-di-iodobenzene, **b** 1,3-di-iodobenzene and **c** 1,4-di-iodobenzene exposure. The exposures were done with the films maintained at 150 K, and exposure is denoted in Langmuirs (L), where 1 L = 1 × 10^{-6} torr s.

The *bars* at the top of each panel are the placement of the calculated molecular orbitals, with the orbital energies rigidly shifted by about 5 eV, approximately consistent with the work function. Binding energies are in terms of E−E$_F$. Adapted with permission from [1]. Copyright (2011) the American Chemical Society
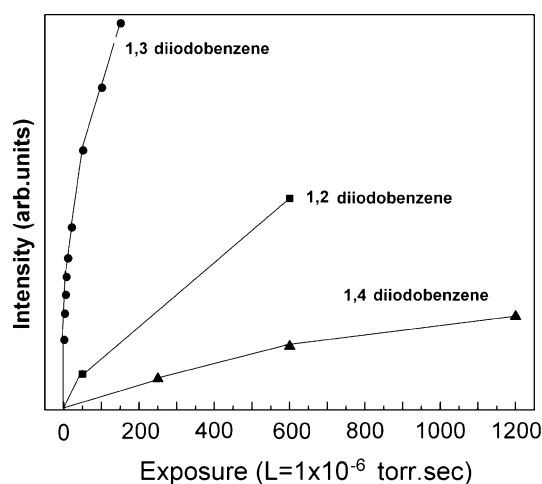

Fig. 7 The iodine 3d$_{5/2}$ core level intensities with increasing exposure of **a** 1,2-di-iodobenzene, **b** 1,3-di-iodobenzene and **c** 1,4-di-iodobenzene exposures to 3 nm thick zwitterion **3** molecular films maintained at 150 K. Exposures are denoted in Langmuirs (L), were 1L = 1×10^{-6} torr × s. Adapted with permission from [1]. Copyright (2011) the American Chemical Society

Fig. 8 Lock and key configuration for the absorption interactions between the di-iodobenzene isomers and the zwitterion **3**; **a** 1,3-di-iodobenzene, **b c** 1,2-di-iodobenzene, d) 1,4-di-iodobenzene. Color code—nitrogen (*dark blue*), carbon (*light blue* and *violet*), iodine (*yellow*), oxygen (*red*). Adapted with permission from [1]. Copyright (2011) the American Chemical Society

preferential isomeric adsorption. Indeed the highest occupied molecular orbital (HOMO) of 1,3-di-iodobenzene bears considerable resemblance to the lowest unoccupied molecular orbital (LUMO) of the core of zwitterion **3** [1]. This molecular recognition phenomenon should therefore be understood within models going beyond simple dipolar interactions, as there are indications that the HOMO of 1,3-di-iodobenzene can strongly hybridize with the LUMO of **3**, if the relative orientation of Fig. 8 is adopted.
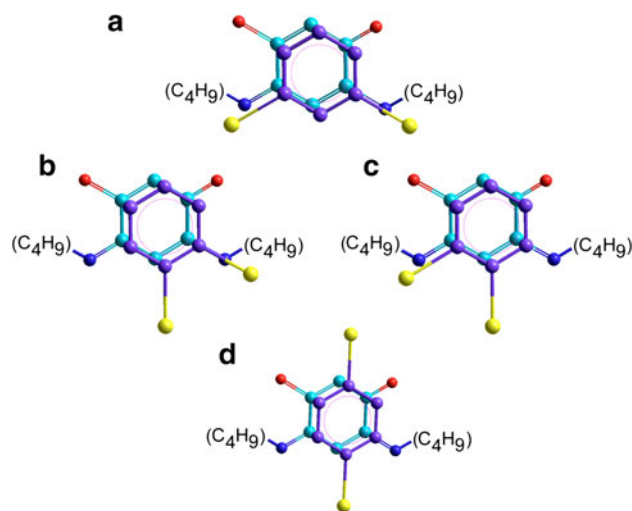
It is clear that there is one orientation of 1,3-di-iodobenzene that favors strong π–π interactions (see Fig. 8), with a concomitant electric dipole co-alignment with the adjacent molecules **3**. The two orientations of 1,2-di-iodobenzene that favor π–π interactions as shown in Fig. 8, with electric dipole co-alignment, with the adjacent molecules **3**, but the alignment is imperfect and the symmetry is not preserved. For 1,4-di-iodobenzene there is one symmetry-preserving orientation that favors π–π interactions

with the adjacent zwitterions, but apart from some induced dipole in the 1,4-di-iodobenzene, there is no expected real dipole alignment (see Fig. 8). If the multiplicity of available favorable orientations based on dipole and π–π interactions is the key factor determining preferential isomeric attachment, then adsorption of 1,2-di-iodobenzene should be preferred, in contradiction with our experimental findings. Our experiments therefore demonstrate that reversible isomer selective adsorption chemistry of small molecules is indeed possible, with preferential adsorption mechanism illustrating that symmetry does matter.

4 The Interaction of a *p*-Benzoquinonemonoimine Zwitterion With Periodically Poled Lithium Niobate

There is yet further evidence that dipole interactions alone do not define the adsorption chemistry of molecular species with large dipoles. Molecules **3** selectively adsorb from solution on periodically poled lithium niobate (LiNbO$_3$) substrates as illustrated in the infra-red spectra-microscopy mapping of this compound on lithium niobate (Fig. 9) [35]. The image shows the distribution of the molecules, using the molecular vibrational mode at 1730 cm^{-1} as a marker of the molecular localization. No vibrational modes specific to LiNbO$_3$ substrate exist in this region of the IR spectrum and LiNbO$_3$ contributions can be excluded.

The general spatial localization (Fig. 9) of this zwitterion **3** suggests that the ferroelectric poling of LiNbO$_3$ either alters the surface chemistry or that there is some dipole–dipole interaction between the zwitterion and ferroelectric domains of the substrate surface. Dipole interactions alone would likely have the zwitterion decorate both "up" and "down" domains of the ferroelectric, so some surface
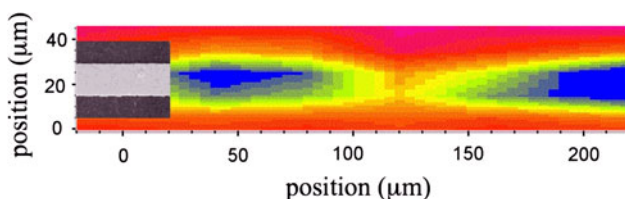

Fig. 9 The spatial localization of the zwitterion **3** using infra-red spectra-microscopy. The resolution in the *y-axis* (*vertical*) direction is limited to several microns. The resolution in the *x-axis* (*horizontal*) direction is 10–15 microns. The inset at left shows the piezoresponse force microscopy phase image of a portion of the periodically poled lithium niobate stripe domains. The IR spatial map was taken using the 1730 cm^{-1} absorption and is in no way characteristic of the lithium niobate substrate. The *less red* and *more blue* seen in the above image, the greater the IR absorption associated with the vibrational mode associated with the zwitterion **3** core to nitrogen group asymmetric stretch at 1730 cm^{-1} (1609 cm^{-1} as calculated). Adapted with permission from [35]. Copyright (2010) the Royal Society of Chemistry

chemistry is certainly implicated in the interaction with the surface of LiNbO$_3$.

5 Summary

Intermolecular electrostatic dipole interactions alone cannot explain our experimental findings on the adsorption of zwitterionic *p*-benzoquinonemonoimine compounds C$_6$H$_2$(···NHR)$_2$(···O)$_2$ on surfaces. Such over simplification will fail to predict the multiplicity of adlayer structures that are observed, not to mention the "lock and key" type of adsorption chemistry possible. The latter is exemplified by di-iodobenzene adsorption studies on molecular films of the zwitterionic *p*-benzoquinonemonoimine **3** which reveal that 1,3-di-iodobenzene adsorption is strongly favored. This isomer of di-iodobenzene shares the same symmetry as the C$_6$ core of the *p*-benzoquinonemonoimine zwitterion compound, suggesting that the frontier molecular orbital symmetry plays a dominant role in preferential isomeric adsorption.

References

1. Zhang Z, Alvira J, Barbosa X, Rosa LG, Routaboul L, Braunstein P, Doudin B, Dowben PA (2011) J Phys Chem C 115:2812–2818
2. Topping J (1927) Proc R Soc A 114:67
3. Levshin NL, Yudin SG, Diankina AP (1997) Mosc Univ Phys Bull (Vestnik Moskovskogo Universiteta Fisika) 52:71–74
4. Martin B, Vizdrik G, Kliem H (2009) J Appl Phys 105:084114
5. Rosa LG, Jacobson PA, Dowben PA (2006) J Phys Chem B 2006(110):7944–7950
6. Dowben PA, Rosa LG, Ilie CC (2008) Z Phys Chem 222:755–778
7. Zhang Z, González R, Díaz G, Rosa LG, Ketsman I, Zhang X, Sharma P, Gruverman A, Dowben PA (2011) J Phys Chem C 115:13041–13046
8. Yun Y, Altman EI (2007) J Am Chem Soc 129:15684
9. Yun Y, Kampschulte L, Liao D, Li M, Altman EI (2007) J Phys Chem C 111:13951
10. Garrity K, Kolpak AM, Ismail-Beigi S, Altman EI (2010) Adv Mater 22:2969–2973
11. Inoue Y, Yoshioka I, Sato K (1984) J Phys Chem 88:1148–1151
12. Inoue Y, Watanabe Y (1993) Catal Today 16:487–494
13. Garra J, Vohs JM, Bonnell DA (2009) Surf Sci 603:1106–1114

14. Zhao MH, Bonnell DA, Vohs JM (2008) Surf Sci 602:2849–2855
15. Zhao MH, Bonnell DA, Vohs JM (2009) Surf Sci 603:284–290
16. Burbure NV, Salvador PA, Rohrer GS (2006) J Am Ceram Soc 89:2943
17. Giocondi JL, Rohrer GS (2001) Chem Mater 13:241
18. Giocondi JL, Rohrer GS (2001) J Phys Chem B 105:8275
19. Kalinin SV, Bonnell DA, Alvarez T, Lei X, Hu Z, Ferris JH, Zhang Q, Dunn S (2002) Nano Lett 2:589
20. Hanson JN, Rodriguez BJ, Nemanich RJ, Gruverman A (2006) Nanotechnology 17:4946
21. Dunn S, Jones PM, Gallardo DE (2007) J Am Chem Soc 129:8724
22. Liu X, Kitamura K, Terabe K, Hatano H, Ohashi N (2007) Appl Phys Lett 91:044101
23. Dunn S, Tiwari D (2008) Appl Phys Lett 93:092905
24. Dunn S, Cullen D, Abad-Garcia E, Bertoni C, Carter R, Howorth D, Whatmore RW (2004) Appl Phys Lett 85:3537
25. Ke C, Wang X, Hu XP, Zhu SN, Qi M (2007) J Appl Phys 101:064107
26. Habicht S, Nemanich RJ, Gruverman A (2008) Nanotechnology 19:495303
27. Haussmann A, Milde P, Erler C, Eng LM (2009) Nano Lett 9:763–768
28. Müller M, Soergel E, Buse K (2003) Appl Phys Lett 83:1824
29. Kunkel DA, Simpson S, Nitz J, Rojas GA, Zurek E, Routaboul L, Doudin B, Braunstein P, Dowben PA, Enders A (2012) Chem Commun 48:7143–7145
30. Rojas G, Simpson S, Chen X, Kunkel DA, Nitz J, Xiao J, Dowben PA, Zurek E, Enders A (2012) Phys Chem Chem Phys 14:4971–4976
31. Onsager L (1936) J Am Chem Soc 58:1486
32. Siri O, Braunstein P (2002) Chem Commun 208–209
33. Braunstein P, Siri O, Taquet JP, Rohmer MM, Bénard M, Welter R (2003) J Am Chem Soc 125:12246–12256
34. Yang QZ, Siri O, Braunstein P (2005) Chem Commun 2660–2662
35. Xiao J, Zhang Z, Wu D, Routaboul L, Braunstein P, Doudin B, Losovyj YB, Kizilkaya O, Rosa LG, Borca CN, Gruverman A, Dowben PA (2010) Phys Chem Chem Phys 12:10329–10340
36. Kong L, Perez Medina GJ, Colón Santana JA, Wong F, Bonilla M, Colón Amill DA, Rosa LG, Routaboul L, Braunstein P, Doudin B, Lee CM, Choi J, Xiao J, Dowben PA (2012) Carbon 50:1981–1986
37. Routaboul L, Braunstein P, Xiao J, Zhang Z, Dowben PA, Dalmas G, DaCosta V, Félix O, Decher G, Rosa LG, Doudin B (2012) J Am Chem Soc 134:8494–8506
38. Fang Y, Nguyen P, Ivasenko O, Aviles MP, Kebede E, Askari MS, Ottenwaelder X, Ziener U, Siri O, Cuccia LA (2011) Chem Commun 47:11255–11257
39. Cahen D, Naaman R, Vager Z (2005) Adv Func Materials 15:1571–1578
40. Natan A, Kronik L, Haick H, Tung RT (2007) Adv Mater 19:4103–4117
41. Taguchi D, Kajimoto N, Manaka T, Iwamoto M (2007) J Chem Phys 127:044703
42. Natan A, Zidon Y, Shapira Y, Kronik L (2006) Phys Rev B 73:193310
43. Yokoyama T, Takahashi T, Shinozaki K, Okamoto M (2007) Phys Rev Lett 98:206102
44. Barth JV, Brune H, Ertl G, Behm RJ (1990) Phys Rev B 42:9307–9318
45. Fukutani K, Wu N, Dowben PA (2009) Surf Sci 603:2964–2971
46. Kim BI (2006) Langmuir 22:9272–9280